Influence of the Composition of Magmatic Melt on the Solubility of Metal Chlorides at Pressures of 0.1–3.0 kbar

V. Yu. Chevychelov and N. I. Suk

Institute of Experimental Mineralogy, Russian Academy of Sciences, Chernogolovka, Moscow oblast, 142432 Russia
e-mail: chev@iem.ac.ru, suk@iem.ac.ru

Abstract—New experimental data are presented for the solubility of metal chlorides in magmatic melts of various compositions at relatively low pressure. The effect of the concentrations of major elements on chlorine solubility was estimated separately for Na, K, Ca, Mg, Sr, and Ba. Chlorine content in the model melts varied at 1250°C within a very wide range from 0.2 to 4.7 wt %. Strong dependence of chlorine solubility on the composition of the magmatic melt was demonstrated. Within the pressure interval from 0.1 to 3.0 kbar, chlorine solubility in Ca-rich melts showed a maximum at about 1 kbar. It was found that the effect of high contents of bivalent alkali earth elements on chlorine solubility in melt is higher than that of monovalent alkali elements. Chlorine solubility in sodium-rich aluminosilicate melt is higher than in potassium-rich composition. The quantitative data obtained in this work can be used for the development of physicochemical models of ore systems, because chlorine is the most important complex-forming agent for the majority of metals.

INTRODUCTION

This paper presents the results of an investigation of the physicochemical conditions under which magmatic melts can dissolve chlorides of metals and be enriched in Cl. It is known that chlorine escapes from melt with fluid becoming the most important complex-forming agent. Subsequently, it can efficiently extract most elements including ore metals from melt or crystalline rock into fluid. Together with H_2O and CO_2, chlorine is one of the major components of magma-derived fluid. Its presence greatly increases the ability of fluid to concentrate and transport ore matter. At relatively high temperature (more than ~800°C) and low pressure (less than ~2 kbar), fluid may fall into the two-phase field and separate into vapor and liquid. This complicates chlorine distribution between the phases of the system. Experimental modeling is the most important source of information on the behavior of chlorine in the process of fluid–magma interaction.

The results of experimental studies on the influence of the composition of aluminosilicate melt on chlorine solubility were considered by many authors (Metrich and Rutherford, 1992; Webster, 1992b; Malinin *et al.*, 1989; Kravchuk and Keppler, 1994; Malinin and Kravchuk, 1995; etc.). This work was reviewed in detail by Malinin and Kravchuk (1995), Webster (1997), and Chevychelov (1999).

At $P_{H_2O} = P_{tot} = 1$ kbar, $T = 830$–850°C, in the presence of ~4 m (NaCl + KCl) fluid, the highest chlorine content of ~0.9 wt % was found in the melt of natural pantellerite (Metrich and Rutherford, 1992). Melts of other compositions contained less Cl: ~0.63 wt % in phonolite and ~0.3 wt % in rhyolite. Metrich and Ruth-

erford (1992) argued that changes in the molar ratios (Na + K)/Al and Al/Si are the main reason of the increase in chlorine content in the sequence rhyolite–phonolite–pantellerite. In our opinion, the main factors responsible for the high chlorine solubility were the high content of iron oxide (~7.9 wt %) in pantellerite melt and the elevated contents of calcium (~2.5 wt %) and iron oxides (2.0 wt %) in the phonolite melt.

Webster (1992b) demonstrated that at $P = 2$ kbar and $T = 800$°C, chlorine solubility increased in model haplogranite melt as its composition changed from subaluminous, through moderately peralkaline or alumina-rich, to strongly peralkaline composition. It was also found that a decrease in Na/(Na + K) reduced chlorine solubility. Kravchuk and Keppler (1994) showed that chlorine solubility in model albite–quartz melts was higher than that in orthoclase–quartz melts. Webster (1992b) supposed that chlorine and sodium complexes are predominant in the structure of water-saturated subaluminous granitic melts. In addition to sodium, chlorine can form complexes with aluminum in alumina-rich melts and with potassium in high-alkali compositions.

Our previous studies (Chevychelov and Chevychelova, 1997; Chevychelov, 1999) concerned the dependence of chlorine solubility on the composition of model Ca-bearing melts (granodiorite, granite, and leucogranite). At a pressure of 1 kbar and a temperature of 1000°C, the highest chlorine contents of ~0.8–0.9 wt % were obtained for the granodiorite composition. Chlorine content declined to ~0.6 and ~0.5 wt % in the granite and leucogranite melts, respectively. Chlorine solubility in all the compositions studied decreased to ~0.15–0.25 wt % at a pressure of 5 kbar

(Chevychelov and Chevychelova, 1997). The observed high chlorine solubilities in the three compositions were explained by the combined influence of relatively high temperature (950–1000°C), low pressure (1 kbar), and melt composition. The increase of chlorine solubility in the sequence leucogranite–granite–granodiorite resulted mainly from the following changes in melt composition: (a) an increase in CaO content, 1.1–1.4–4.0 wt %, respectively; (b) a decrease in agpaitic coefficient, $(Na_2O + K_2O)/Al_2O_3$, 0.99–0.98–0.84; and (c) a decrease in SiO_2 content, 75.9–73.2–67.9 wt % (Chevychelov, 1999).

Gorbachev and Khodarevskaya (1995) and Khodarevskaya and Gorbachev (1993) reported higher chlorine solubility in andesitic (~1 wt %) and basaltic (~1.25 wt %) melts in comparison with silicic compositions at P = 1–2 kbar and T = 1100°C. These authors studied chlorine solubility and partitioning between water–chloride fluid and basic and intermediate melts within a wide pressure interval, 1.0–11.5 kbar.

There are few data on chlorine solubility in anhydrous ("dry") aluminosilicate melts. At P_{tot} = 2 kbar and T = 1200–1250°C, chlorine solubility under "dry" conditions is ~1.1–1.8 wt % in intermediate alkaline melts (~56.5–60.0 wt % SiO_2) and increases to 2.0–2.8 wt % in alkaline basic melts (~49.0–56.5 wt % SiO_2) (Suk, 1997). A.V. Kosyakov studied the solubilities of KCl, NaCl, $MgCl_2$, $CaCl_2$, $FeCl_3$, and $AlCl_3$ in tholeiitic basalt melt under "dry" conditions (Litvin *et al.*, 1986). The experiments were carried out at P = 30 kbar and T = 1500°C. In each experiment, a mixture of basalt with one of the chlorides was used. This resulted in the enrichment of the melt in the respective metal. The dependence of Cl solubility in melt on the concentration of each of these metals was estimated. The concentration of Cl in quenched aluminosilicate glasses was (wt %) 3.0 in experiments with KCl; 4.4, with NaCl; 5.3, with $AlCl_3$; 9.5, with $CaCl_2$; and 9.9, with $FeCl_3$. Malinin *et al.* (1989) demonstrated similar behavior of Cl in hydrous salt and "dry" systems, more specifically, the identical character of the influence of oxide component composition on Cl solubility.

The influence of pressure on chlorine solubility in silicic igneous melts was studied mainly within 2–8 kbar and T = 700–1000°C (Kilinc and Burnham, 1972; Shinohara *et al.*, 1989; Malinin *et al.*, 1989; Webster, 1992a; etc.). The lowest chlorine solubility was established at a pressure of about 5–6 kbar for melts of acid, intermediate, and basic compositions (Gorbachev and Khodorevskaya, 1995). The experimental data at lower (0.5–2.0 kbar) pressure are limited (Shinohara *et al.*, 1989; Metrich and Rutherford, 1992; Webster, 1997). Metrich and Rutherford (1992) demonstrated that chlorine solubility in pantellerite melt increased with decreasing pressure in the sequence 2.0–1.4–1.0–0.5 kbar from 0.5–0.71–0.9–0.96 wt %. It was not clear if chlorine solubility would continue increasing with decreasing pressure below 1.0–0.5 kbar, or the pressure

dependency of chlorine solubility would pass through a maximum. Kravchuk *et al.* (1998) showed an increase in the influence of melt composition (Na_2O content) on chlorine solubility with decreasing pressure in the range from 7.0 to 1.5 kbar.

In general, an increase in experimental temperature enhances chlorine solubility in aluminosilicate melts. Webster (1992a) showed this regularity for subaluminous and peralkaline haplogranite melts at T = 800 and 1000°C and P = 2 kbar. A similar dependency was obtained by Chevychelov (1999) for the melts of granodiorite, granite, and leucogranite compositions at T = 770–1000°C and pressures of 1 and 5 kbar. At P = 5 kbar and initial 1 m HCl solution, chlorine solubility in tholeiitic basalt melt increased by a factor of three (from 0.6 to 1.7 wt %) as temperature changed from 1100 to 1200°C but, for unknown reason, remained constant at a further increase in temperature up to 1300°C (Gorbachev and Khodorevskaya, 1995).

Thus, although the regularities of chlorine solubility in aluminosilicate melts were repeatedly studied, a number of issues remain to be explained. Most studies were carried out at pressures higher than 1.5–2.0 kbar. There are only limited and fragmentary data for P < 1 kbar, when chlorine solubility increases most rapidly. Among silicic melts, haplogranite SiO_2–Al_2O_3–Na_2O–K_2O compositions enriched in alkalis [(Na + K)/Al ≥ 1] were most thoroughly studied, whereas the influence of some important rock-forming components including Ca, Mg, and Fe was almost never estimated in experiments. The influence of silica content in the melt modeling natural compositions from strongly acid (leucogranite) to alkaline and basic is also not adequately known. This paper presents new experimental data on the solubility of chlorides of alkali and alkali earth metals in magmatic melts within a wide range of compositions at relatively low pressure. The influence of major component contents on Cl solubility in melt was studied separately for K, Na, Ca, Mg, Sr, and Ba. In addition to the concentrations of particular elements, the solubility of chlorine in aluminosilicate melt is certainly affected by a number of other factors. Among them are differences in the structures of compositionally different melts, e.g., different degrees of polymerization of silicic and basic melts.

EXPERIMENTAL CONDITIONS AND STARTING MATERIALS

Experiments were conducted at T = 1250°C and pressures from 100 to 3000 bar in an internally heated gas pressure vessel (UVGD-10000). The high experimental temperature was dictated by the high liquidus temperatures of melts at relatively low pressure and the presence of alkali earth elements, Ca, Mg, Sr, and Ba in the melt. The duration of experiments was 4.0–4.5 days. Chevychelov (1999) and Chevychelov and Epel'baum (1985) demonstrated that under the experimental P–T

Table 1. Compositions of starting materials (wt %) mixed from minerals, chlorides, and water

Compo-nent	Na-d/3*	Ca-d/3*	Albt/3*	Ortc/3*	Ca-b/3*	Na-b/3*	Ca-s/4*	Mg-s/4*	NM-g/4*	NC-d/4*	NS-d/4*	NB-d/4*
Qtz	12.6–13.4	23.5–24.5	1.8–2.0	1.8–1.9	–	–	–	–	–	$\frac{13.2}{13.3}$	$\frac{13.2}{13.2}$	$\frac{13.2}{13.2}$
Or	–	–	–	67.8–70.7	–	–	–	–	–	–	–	–
Ab	37.6–39.3	10.8–11.2	60.5–63.3	–	16.4–16.6	22.9–24.3	$\frac{47.2}{49.0}$	$\frac{47.2}{47.4}$	37.9	$\frac{28.3}{30.5}$	$\frac{28.3}{26.4}$	$\frac{28.3}{30.1}$
An$_{80}$	19.7–20.6	36.2–37.3	–	–	31.8–33.7	–	–	–	–	$\frac{24.5}{22.8}$	–	–
SrAl$_2$Si$_2$O$_8$	–	–	–	–	–	–	–	–	–	–	$\frac{24.5}{26.3}$	–
BaAl$_2$Si$_2$O$_8$	–	–	–	–	–	–	–	–	–	–	–	$\frac{24.5}{22.6}$
Ne	–	–	7.1–7.4	–	–	46.4–48.7	–	–	–	–	–	–
Wo	–	–	–	–	21.3–22.4	–	$\frac{18.9}{16.9}$	–	–	–	–	–
En	–	–	–	–	–	–	$\frac{18.9}{19.0}$	28.4	–	–	–
NaCl	10.9–11.5	3.6–4.1	19.4–20.5	–	3.5–3.9	19.2–20.6	$\frac{24.5}{24.5}$	$\frac{24.5}{24.7}$	24.6	$\frac{24.6}{24.8}$	$\frac{24.6}{24.5}$	$\frac{24.6}{24.5}$
KCl	–	–	–	20.2–20.6	–	–	–	–	–	–	–	–
CaCl$_2$	8.1–9.3	15.2–16.8	–	–	14.4–16.6	–	–	–	–	–	–	–
H$_2$O	6.5–10.3	6.7–9.6	6.9–10.9	6.9–9.8	7.6–10.3	6.4–11.4	$\frac{9.4}{9.6}$	$\frac{9.4}{8.9}$	9.1	$\frac{9.4}{8.6}$	$\frac{9.4}{9.6}$	$\frac{9.4}{9.6}$

* Full names of the starting materials are given in the text. The denominator shows the number of table containing information on the sample. Dashes in this and following tables denote the absence of the component in the sample.

Columns Na-d/3, Ca-d/3, Albt/3, Ortc/3, Ca-b/3, and Na-b/3 show the initial compositions of experiments at P = 0.3, 0.6, 1.0, 2.0, and 3.0 kbar. H$_2$O content increases on average from ~7.0% at 0.3 and 0.6 kbar to ~10.3% at 3.0 kbar; the percentages of other components decrease accordingly. The concentration of H$_2$O in experiments at P = 0.1 kbar averages at ~3.4%. In columns Ca-s/4, Mg-s/4, NC-d/4, NS-d/4, and NB-d/4, the numerator shows the initial composition of the experiment at P = 1.0 kbar, and denominator, at P = 3.0 kbar.

parameters such exposures are sufficient to attain conditions close to equilibrium.

A carefully ground mixture of minerals and Na, K, and Ca chlorides was loaded together with distilled water into a platinum capsule, 3 mm in diameter, 25–30 mm long, and 0.1 mm in wall thickness. The charge with water amounted at 50–55 mg. The following proportions were maintained: ~66–72% of minerals, ~20–25% of chlorides, and ~5–10% of water. The compositions of the initial mixtures are given in Table 1. Natural and synthetic minerals and glasses were used: *Qtz*, amorphous silica; *Or*, potassium feldspar; *Ab*, albite; *An$_{80}$*, homogeneous glass of the bytownite composition; *Ne*, nepheline; *Wo*, wollastonite; SrAl$_2$Si$_2$O$_8$, Sr feldspar; BaAl$_2$Si$_2$O$_8$, celsian; and *En*, enstatite (Table 2).

The choice of model compositions for our investigation aimed at determining the influence of individual components in melt composition on chlorine solubility. Four-component aluminosilicate melts were used with relatively constant SiO$_2$ and Al$_2$O$_3$ and variable concentrations of two other components. The later were Na$_2$O and CaO, Na$_2$O and MgO, Na$_2$O and SrO, or Na$_2$O and BaO. In addition, acid and basic compositions with different SiO$_2$ contents and three-component compositions approaching albite and orthoclase were studied. The compositions lie within the subaluminous [molar ratio Al$_2$O$_3$/(CaO + Na$_2$O + K$_2$O) ~ 1] and metaluminous (A/CKN < 1) fields (Johannes and Holtz, 1996). The normative compositions of the melts corresponded to dacite, syenite, and alkali basalt.

The compositions of experimental aluminosilicate glasses were determined on the Camebax electron microprobe with an energy dispersive system Link-10000 in the Institute of Experimental Mineralogy, Russian Academy of Sciences. The counting time was (τ) = 70 s; probe diameter, ~2–5 μm; and U = 15 kV. Five to ten spots were analyses in different parts of each sample, and the average contents were subsequently

Table 2. Chemical compositions of initial silicate minerals (wt %) analyzed by an electron microprobe

Component	SiO_2	Al_2O_3	FeO	MnO	MgO	CaO	SrO	BaO	Na_2O	K_2O
Natural minerals										
Or	65.09	17.97	–	–	–	–	–	–	0.87	16.07
Ab	67.38	19.82	–	–	–	0.27	–	–	12.39	0.14
Ne	44.75	32.97	0.n	–	–	–	–	–	15.70	6.58
Wo	51.76	–	0.66	0.30	–	47.28	–	–	–	–
En	59.69	0.16*	0.57	–	39.58	–	–	–	–	–
Synthetic minerals and glasses										
Qtz	100	–	–	–	–	–	–	–	–	–
An_{80}	45.22	35.04	–	–	–	16.71	–	–	2.97	0.06*
$SrAl_2Si_2O_8$	36.68	30.23	–	–	–	–	33.09	–	–	–
$BaAl_2Si_2O_8$	31.16	27.69	–	–	–	–	–	41.15	–	–

Note: Full names of minerals are given in the text. *Qtz* is amorphous SiO_2; An_{80}, homogeneous glass obtained from oxides at $T = 1600°C$ (provided by A.R. Kotel'nikov). $SrAl_2Si_2O_8$ and $BaAl_2Si_2O_8$ are fully crystallized samples obtained by the method of solid-state synthesis from oxide and carbonate mixtures (provided by A.M. Koval'skii). *Wo* and *En* were provided by G.P. Zaraiskii.
* Concentrations below the analytical error (2σ).

used. In order to minimize sodium loss during measurements, the analysis was performed by scanning over an area or 10×10 μm. Rare aluminosilicate crystals, which occurred in some experiments, were also analyzed. Concentrations were calculated using the ZAF correction procedure. The method of chlorine analysis was described in detail by Chevychelov (1999). The error of Cl analysis (σ_{Cm}) was 0.04–0.06 wt %, and the detection limit (C_{min}) was ≤0.1 wt % at a probability of 85%. The analytical uncertainties for other elements were no higher than 0.1–0.2 wt %. Chevychelov (1999) demonstrated adequate consistency of chlorine contents measured by the energy dispersive system (Link 1000) and a more sensitive wavelength dispersion spectrometer.

The obtained chemical compositions were recalculated to some characteristic molar and atomic ratios and contents and normative CIPW components.

EXPERIMENTAL RESULTS

The initial aluminosilicate–chloride mixture separated into two liquids during the experiments, aluminosilicate and chloride. The aluminosilicate melt quenched after the experiment forming transparent homogeneous glass contacting a fine-crystalline quench chloride aggregate (Fig. 1). As a less dense phase, the salt aggregate usually occurred in the upper part of the capsule and was distinctly separated from the aluminosilicate glass. The aluminosilicate glasses contained no crystal phases except for four experiments, which are described below.

Ca–Na–K-bearing Compositions

Table 3 presents results for SiO_2–Al_2O_3–CaO–Na_2O–K_2O–MeCl–H_2O compositions, where Me is Na, Ca, or K. Six compositions were selected; they are conventionally referred to as Na-dacite (Na-d), Ca-dacite (Ca-d), albitite (*Albt*), orthoclasite (*Ortc*), Ca-basalt (Ca-b), and Na-basalt (Na-b). The experiments with these compositions were conducted at $T = 1250°C$ and six different pressures, 0.1, 0.3, 0.6, 1.0, 2.0, and 3.0 kbar. Chlorine content in the melt increased significantly with increasing calcium content. The chlorine content of the albitite glass was about twice as high as that of orthoclasite.

Two experimental series were performed at $P = 1$ kbar. Minor differences between the compositions of melts from these two experimental series affected Cl content. For instance, a decrease in CaO content from 24.27 to 22.69 wt % and an increase in Al_2O_3 from 18.01 to 21.37 wt % in the Ca-b composition resulted in a decrease in Cl content from 4.71 to 3.86 wt %. In the Na-d composition, a decrease in CaO from 5.17 to 3.96 wt % and an increase in Na_2O from 7.97 to 9.04 wt % changed Cl content from 1.41 to 1.27 wt %. Thus, chlorine concentration in the melt increases with increasing CaO content.

Figure 2 shows, as an example, the compositions of model melts after the experiment at a pressure of 3 kbar on the Na_2O–K_2O–CaO and Qtz–(Ab + Or + Ne)–(An + Wo) diagrams. As is seen in Fig. 2a, five Ca–Na-bearing compositions and one K-rich composition were studied. The normative compositions of the glasses are given in Table 3 and Fig. 2b.

The chlorine content of the aluminosilicate glasses studied varies from 0.2 to 4.7 wt %. The analysis of the experimental data suggests that the influence of changes in melt composition on chlorine content is
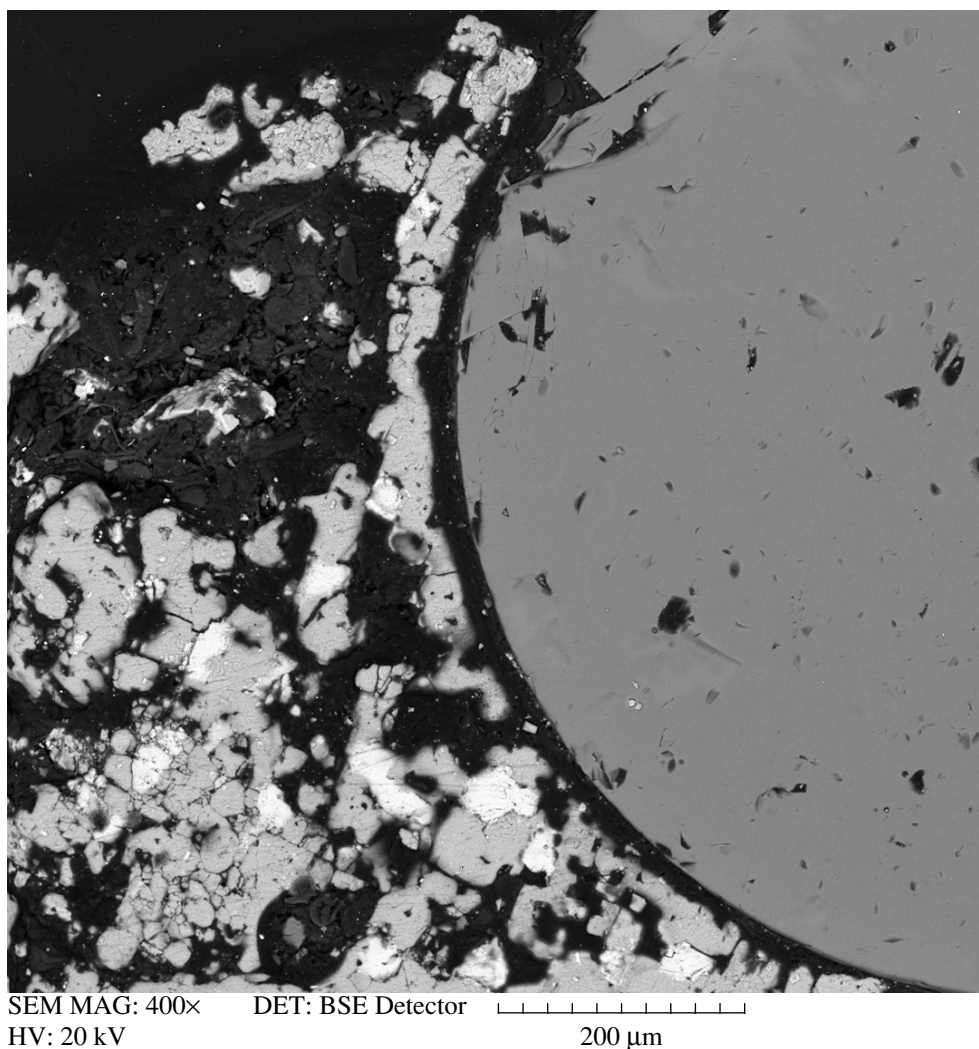
SEM MAG: 400×   DET: BSE Detector
HV: 20 kV   200 μm

Fig. 1. Back-scattered electron image of aluminosilicate and chloride liquid immiscibility, $P = 0.1$ kbar, $T = 1250$°C, magnification of ×400.

stronger than that of pressure (Fig. 3). For instance, under the same P–T conditions, the Cl content of Ca-basalt melt is higher by a factor 10–15 than that of orthoclasite melt. Within a pressure interval from 0.1 to 3.0 kbar, Cl content in glass of a given composition varies much less significantly, by a factor of no more than 1.5–2.0. Within the pressure interval studied, chlorine solubility passes through a maximum. It is clearly manifested in the melts of Ca-basalt and Ca-dacite at about 1 kbar.

In the compositional sequence albitite–Na dacite–Ca dacite, CaO content increases, Na_2O decreases, Al_2O_3 remains constant, and SiO_2 slightly decreases (Fig. 4). These changes in melt composition are accompanied by an increase in chlorine content. At the transition from the Na-basalt to Ca-basalt composition, CaO content increases sharply, while Na_2O, Al_2O_3, and other components significantly decrease (Fig. 5). This results

in an increase in chlorine content by a factor of almost five, from 1.0 to 4.7 wt %.

The homogeneity of the distribution of chlorine and other chemical elements within the volume of aluminosilicate melts was checked on a CamScan MV 2300 microprobe. The aluminosilicate melt quenched after experiments into a transparent homogeneous glass. Figure 6 displays the intensities of Si, Ca, Al, O, Cl, and Na radiation along a profile across two gas "inclusion–bubbles" in the Ca-basalt sample ($P = 1$ kbar) with the highest chlorine content (~4.71 wt %). It should be noted that such inclusion–bubbles are very rare in the quench glasses of our experiments. This image was obtained at the highest possible magnification of ×4000 and a resolution of a few micrometers (size of excitation zone of the electron microprobe). Figure 6 shows that within the main glass volume, the intensities of radiation of all major elements remain constant, whereas all intensities fall dramatically in the gas inclu-

Table 3. Electron microprobe analyses (wt %), calculated molar ratios, and normative compositions (wt %) of aluminosilicate glasses obtained in experiments in the system SiO_2 –Al_2O_3 –CaO –Na_2O –K_2O –$MeCl$ –H_2O at pressures from 0.1 to 3.0 kbar, a temperature of 1250°C, and run durations of 4.0–4.5 days

Compo-nent	P = 0.1 kbar						P = 0.3 kbar					P = 0.6 kbar				
	Na-d	Ca-d	Albt	Ortc	Ca-b	Na-b	Na-d	Albt	Ortc	Ca-b	Na-b	Na-d	Ca-d	Albt	Ortc	Na-b
SiO_2	65.40	61.81	67.47	67.64	49.62	53.66	64.84	67.62	67.07	51.09	54.11	65.16	62.02	66.85	67.42	53.39
Al_2O_3	19.29	19.72	20.08	16.80	19.48	27.83	19.86	19.60	17.16	18.79	27.49	19.95	20.23	20.08	17.10	27.88
FeO	–	–	–	–	0.10*	0.14*	–	–	–	0.06*	0.14*	–	–	–	–	0.13*
CaO	5.71	12.13	0.19	–	23.56	0.10*	5.23	0.04*	–	22.78	0.09*	5.01	11.12	0.06*	–	0.16
Na_2O	8.39	4.55	11.32	1.30	4.04	15.50	8.75	11.76	1.13	3.84	15.24	8.42	4.44	11.90	1.38	15.33
K_2O	0.03*	0.02*	0.35	14.05	0.07*	2.06	0.09	0.32	14.40	0.13	2.14	0.16	0.10*	0.41	13.81	2.25
Cl	1.18	1.77	0.59	0.21	3.13	0.71	1.23	0.66	0.24	3.31	0.79	1.30	2.09	0.70	0.29	0.86
Total	100	100	100	100	100	100	100	100	100	100	100	100	100	100	100	100
A/CNK**	0.798	0.667	1.037	0.968	0.393	0.997	0.827	0.995	0.983	0.392	0.998	0.863	0.732	0.998	0.994	0.998
ANC/S**	0.690	0.729	0.679	0.330	1.129	1.173	0.709	0.679	0.334	1.057	1.146	0.694	0.715	0.700	0.338	1.175
Ca**	2.09	4.54	0.07	–	9.20	0.04	1.92	0.01	–	8.89	0.03	1.84	4.16	0.02	–	0.06
SiO_2**	70.15	65.76	73.36	76.64	51.77	60.95	69.89	73.54	76.29	53.21	61.40	70.26	66.09	72.79	76.44	60.77
C/S**	0.094	0.210	0.003	–	0.509	0.002	0.086	0.001	–	0.478	0.002	0.082	0.192	0.001	–	0.003
Qtz	7.33	15.41	–	8.39	–	–	4.99	–	6.53	–	–	6.89	16.75	–	7.09	–
Or	0.18	0.12	2.08	83.58	0.43	12.29	0.54	1.90	85.55	0.80	12.78	0.96	0.60	2.44	82.00	13.44
Ab	71.76	39.15	96.23	8.03	19.82	34.37	74.87	95.71	7.92	25.98	35.84	72.10	38.33	92.67	10.91	32.64
An	15.04	33.89	0.95	–	35.93	0.26	14.81	–	–	34.78	0.26	16.36	35.68	0.16	–	0.60
Ne	–	–	–	–	–	52.98	–	2.30	–	4.12	51.04	–	–	4.67	–	53.23
Crn	–	–	0.74	–	–	–	–	–	–	–	–	–	–	–	–	–
Wo	5.69	11.44	–	–	8.38	0.10	4.79	0.08	–	34.32	0.08	3.69	8.64	0.06	–	0.08

Table 3. (Contd.)

Component	P = 1.0 kbar					P = 2.0 kbar					P = 3.0 kbar					
	Na-d	Ca-d	Albt	Ca-b	Na-b	Na-d	Albt	Ortc	Ca-b	Na-b	Na-d	Ca-d	Albt	Ortc	Ca-b	Na-b
SiO_2	65.80/66.05	60.84/62.15	67.76/67.27	49.74/48.83	54.69/53.52	66.33	67.56	67.37	48.91	53.87	66.50	63.20	67.62	67.47	49.53	53.86
Al_2O_3	19.44/19.63	20.19/20.24	19.69/19.70	18.01/21.37	27.02/27.72	19.72	19.83	17.15	20.35	27.94	19.88	21.44	19.85	16.96	19.54	27.87
FeO	–	–	–	0.18*/0.12*	0.30/0.23*	–	–	–	0.15*	0.22*	–	–	–	–	0.27	0.24
CaO	5.17/3.96	12.00/11.75	0.15/0.07*	24.27/22.69	0.45/0.13	5.25	0.09*	–	23.93	0.12*	5.33	10.40	0.08*	–	24.39	0.09*
Na_2O	7.97/9.04	4.48/3.45	11.21/11.83	2.98/3.08	14.72/15.54	7.26	11.40	1.03	2.85	15.05	7.03	3.03	11.39	1.06	2.55	15.16
K_2O	0.21/0.05*	0.16/0.05*	0.36/0.36	0.11/0.05	1.82/1.97	0.03*	0.35	14.11	0.03*	1.75	0.03*	0.04*	0.34	14.13	0.05*	1.79
Cl	1.41/1.27	2.33/2.36	0.83/0.77	4.71/3.86	1.00/0.89	1.41	0.77	0.34	3.78	1.05	1.23	1.89	0.72	0.38	3.67	0.99
Total	100/100	100/100	100/100	100/100	100/100	100	100	100	100	100	100	100	100	100	100	100
A/CNK**	0.855/0.887	0.687/0.747	1.031/0.986	0.367/0.461	1.001/0.992	0.916	1.028	1.011	0.422	1.040	0.934	0.897	1.031	0.995	0.402	1.031
ANC/S**	0.667/0.680	0.745/0.694	0.666/0.687	1.066/1.136	1.113/1.176	0.647	0.675	0.330	1.128	1.155	0.643	0.669	0.674	0.327	1.092	1.157
Ca**	1.90/1.45	4.51/4.41	0.05/0.02	9.57/8.88	0.16/0.05	1.93	0.03	–	9.39	0.04	1.96	3.88	0.03	–	9.59	0.03
SiO_2 **	70.71/71.17	64.67/66.09	73.56/73.15	50.99/51.19	61.71/60.81	71.31	73.50	76.51	51.02	61.12	71.63	67.87	73.60	76.52	51.52	61.13
C/S**	0.084/0.064	0.211/0.203	0.002/0.001	0.523/0.498	0.009/0.003	0.085	0.001	–	0.524	0.002	0.086	0.176	0.001	–	0.528	0.002
Qtz	9.73/6.44	14.25/21.30	0.98/–	–	–	14.08	–	7.38	–	–	15.17	25.13	–	7.65	–	–
Or	1.26/0.30	0.97/0.30	2.15/2.14	0.68/0.31	10.91/11.78	0.18	2.09	83.74	0.18	10.48	0.18	0.24	2.03	83.96	0.31	10.72
Ab	68.32/77.39	38.77/29.86	95.54/94.29	22.74/20.03	40.40/34.77	62.24	96.73	8.73	19.20	39.32	60.15	26.10	96.96	8.40	21.08	38.62
An	16.86/12.98	35.29/40.50	0.75/–	37.22/46.12	2.26/0.05	21.41	0.45	–	44.34	0.60	22.85	45.59	0.40	–	43.38	0.45
Ne	–	–	–/3.42	2.03/3.84	46.42/53.14	–	0.20	–	3.19	48.51	–	–	–	–	0.73	49.38
Crn	–	–	0.59/–	–	–	–	0.54	0.15	–	1.08	–	–	0.60	–	–	0.83
Wo	3.83/2.89	10.73/8.03	–/0.15	37.33/29.70	–/0.25	2.10	–	–	33.10	–	1.64	2.93	–	–	34.49	–

Note: Average concentrations are given for 5–10 microprobe analyses for every experiment. Two experimental series were carried out at P = 1 kbar. Numerators show the compositions of glasses from the first series, and denominators, from the second series. All iron is in FeO form.

* Concentration below the analytical error (2σ).

** A/CNK is the molar ratio $Al_2O_3/(CaO + Na_2O + K_2O)$; ANC/S, atomic ratio (Al + Na + Ca)/Si; Ca, concentration of Ca, at. %; SiO_2, concentration of SiO_2 in mol %; and C/S, molar ratio CaO/SiO_2.
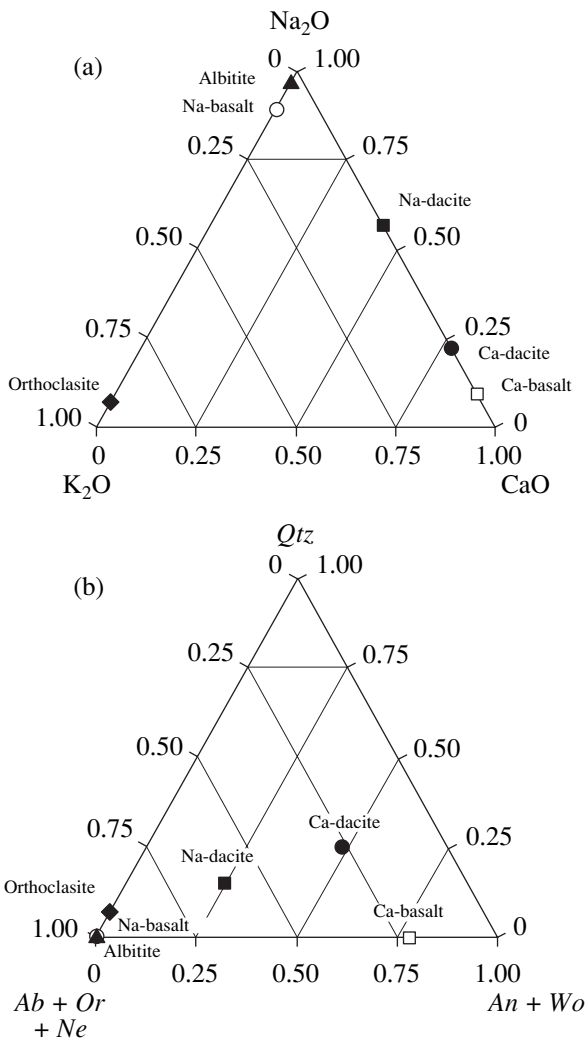
Fig. 2. Compositions of quenched aluminosilicate glasses modeling Na-dacite, Ca-dacite, albitite, orthoclasite, Ca-basalt, and Na-basalt ($P = 3.0$ kbar and $T = 1250°C$): (a) $Na_2O–K_2O–CaO$ and (b) $Qtz–(Ab + Or + Ne)–(An + Wo)$ diagrams.
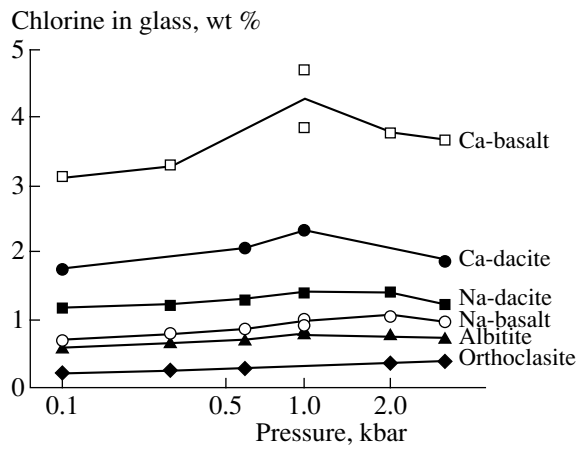

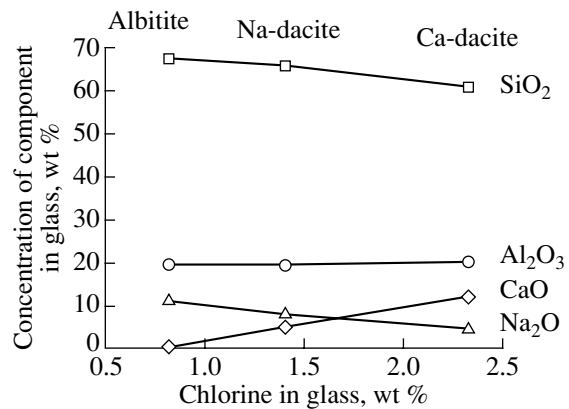**Fig. 3.** Dependence of chlorine content in melts on experimental pressure and melt composition.

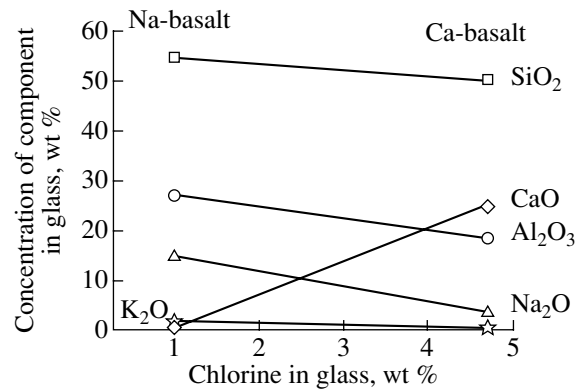**Fig. 4.** Chlorine contents in the melts of Na-dacite, Ca-dacite, and albitite compositions at $P = 1.0$ kbar.

Fig. 5. Chlorine contents in the model melts of Na-basalt and Ca-basalt compositions at $P = 1.0$ kbar.

sion–bubbles. In contrast, the intensity of carbon (C), which was used for sample coating, increases. Carbon was probably accumulated in these cavities during coating. The detailed examination of this and other samples of quench glasses did not reveal crystalline phases, which could have been identified as chlorides. Thus, it can be supposed that at a resolution of a few micrometers, chlorine was homogeneously distributed in the volume of aluminosilicate melts in our experiments.

The molar ratios $Al_2O_3/(CaO + Na_2O + K_2O)$ and CaO/SiO_2 and CaO content provide major controls on Cl contents in Ca–Na-bearing compositions (Figs. 7–9). At $P = 1$ kbar, an increase in chlorine content in these melts is accompanied by a proportional decrease in the former ratio from ~1 to ~0.37, an increase in the latter ratio from ~0.001 to ~0.52, and a proportional increase

in Ca content from ~0.02 to ~9.6 at. %. These regularities are consistent with the results of Chevychelov (1999). However, for the selected group of compositions, the atomic ratio $(Al + Na + Ca)/Si$ or SiO_2 content show poor correlations with chlorine concentration in the melt.

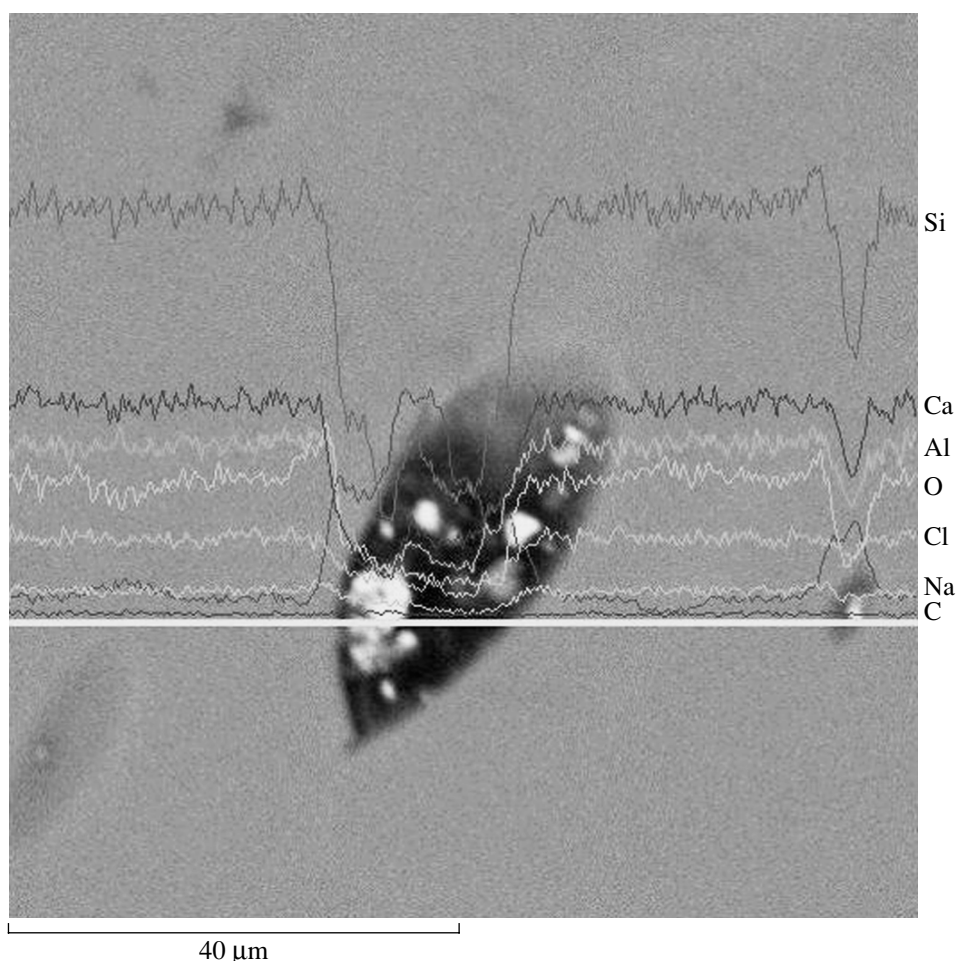**Fig. 6.** Back-scattered electron image of the Ca-basalt sample (P = 1 kbar and T = 1250°C) containing the maximum amount of chlorine (~4.71 wt %).
Intensities of Si, Ca, Al, O, Cl, Na, and C radiation are shown along the profile (white horizontal line). Magnification is ×4000.

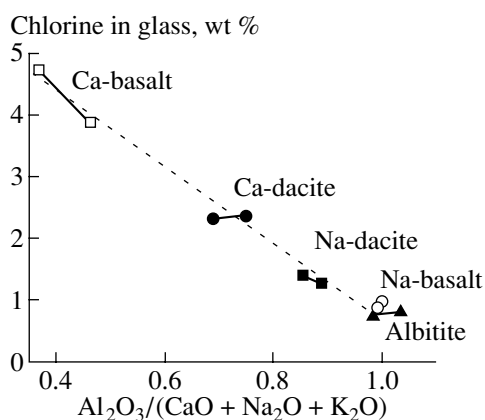**Fig. 7.** Dependence of chlorine content on the molar ratio $Al_2O_3/(CaO + Na_2O + K_2O)$ of melt for Ca- and Na-bearing compositions.
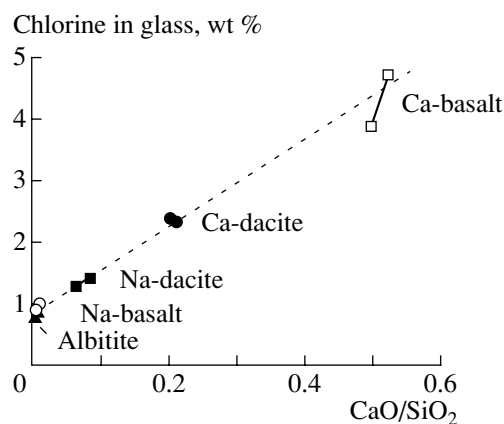
Fig. 8. Dependence of chlorine content on the CaO/SiO_2 molar ratio of melt for Ca- and Na-bearing compositions.

Mg–Ca–Sr–Ba–Na-bearing Compositions

Table 4 shows results obtained for the compositions $SiO_2–Al_2O_3–MgO–CaO–SrO–BaO–Na_2O–NaCl–H_2O$. Six compositions were selected and are conventionally referred to as Ca-syenite (Ca-s), Mg-syenite (Mg-s), Na–Mg-granite (NM-g), Na–Ca-dacite (NC-d), Na–Sr-dacite (NS-d), and Na–Ba-dacite (NB-d). These experiments were conducted at pressures of 1.0 and 3.0 kbar.
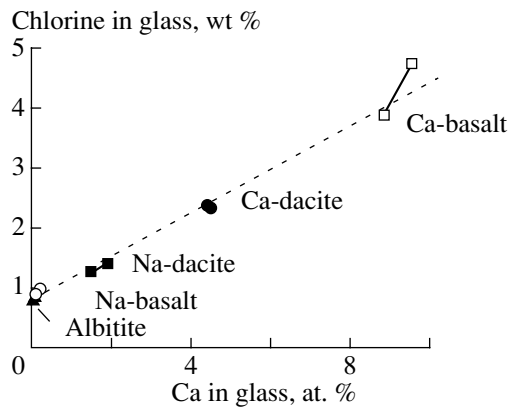
Fig. 9. Dependence of chlorine content on the Ca content of melt for Ca- and Na-bearing compositions.
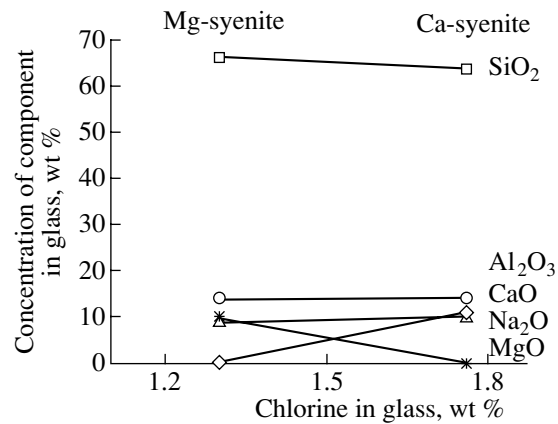

Fig. 10. Chlorine content in the model melts of Mg-syenite and Ca-syenite compositions at $P = 3.0$ kbar.

Glasses from four experiments (marked in Table 4) contained ~5–10 vol % of silicate crystals. At $P = 1$ kbar, Mg-s contained enstatite and olivine; NS-d, crystals of Sr feldspar; NB-d, crystals of $BaAl_2Si_2O_8$; and NM-g contained forsterite crystals at $P = 3$ kbar.

The comparison of MgO- and CaO-rich syenite melts shows higher Cl content in Ca composition (Fig. 10). Figure 11 compares the relative effects of CaO, SrO, and BaO on chlorine solubility in the dacite melt. The highest chlorine content was found in Na–Ca dacite, which contained relatively low amount (13.8 wt %) of normative anorthite. It is followed by the Na–Sr and Na–Ba dacite compositions, and the lowest chlorine content was determined in the albitite composition.

DISCUSSION

The data on the concentration of chlorine in model aluminosilicate melts of varying composition can be regarded as Cl solubility because (1) the systems under investigation closely approached equilibrium under experimental conditions (Chevychelov, 1999; Chevychelov and Epel'baum, 1985) and (2) under experimental conditions ($P = 1$ kbar and lower and $T = 1250°C$), the aluminosilicate melts were water-saturated. The latter condition is important because of the coupling of Cl and H_2O contents in igneous melts (Webster, 1997). Chevychelov et al. (2003) reported the results of an investigation of joint Cl and H_2O solubility in a model granodiorite melt at 1 kbar, 1000°C, and bulk chloride concentrations in fluid varying from 0 to ~98 wt %. They established essentially constant chlorine content in the granodiorite melt within experimental uncertainties, which did not depend on the bulk composition of fluid at salt concentrations higher than 15% MeCl. The bulk content of water in melt was also constant.

The solubility of H_2O in aluminosilicate melt is roughly estimated as ~0.5 to ~8.0 wt % depending on P–T parameters and melt composition (Johannes and Holtz, 1996; Kadik et al., 1971). The amount of water

loaded into the platinum capsule was sufficient for the saturation of the aluminosilicate melt in each particular experiment. At $P = 1$ kbar and lower and $T = 1250°C$, chloride fluid probably separates into two phases, water-dominated and salt melt–solution. Although high-pressure and high-temperature phase relations are not known in detail for such complex systems as $NaCl + CaCl_2 + H_2O$ and others, we believe on the basis of a rough estimate that the amount of water introduced into the initial material was sufficiently high in our experiments to provide the occurrence of minor amounts of water-dominated fluid phase coexisting with the salt phase. It is highly probable that this phase composed of almost pure water. In such a case, the aluminosilicate melt can be considered as water-saturated.

Our results suggest rather strong influence of melt composition (concentrations of major rock-forming components) on chlorine solubility. It is reasonable to suppose that this influence is especially strong at relatively low pressures (Kravchuk et al., 1998) and is
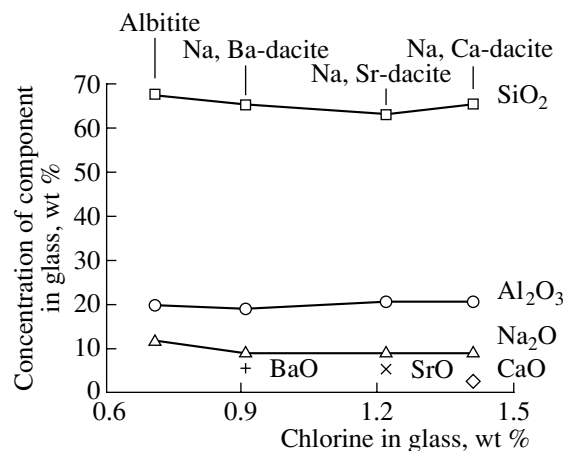

Fig. 11. Chlorine contents in the melts of Na–Ca-dacite, Na–Sr-dacite, Na–Ba-dacite, and albitite compositions at $P = 3.0$ kbar.

Table 4. Electron microprobe analyses (wt %), calculated molar ratios, and normative compositions (wt %) of aluminosilicate glasses obtained in experiments in the system SiO_2 –Al_2O_3 –MgO –CaO –SrO –BaO –Na_2O–$NaCl$ –H_2O at pressures of 1.0 and 3.0 kbar, a temperature of 1250–1270°C, and run durations of 3–4 days

Component	P = 1.0 kbar					P = 3.0 kbar					
	Ca-s	Mg-s[1]	NC-d	NS-d[1]	NB-d[1]	Ca-s	Mg-s	NM-g[1]	NC-d	NS-d	NB-d
SiO_2	63.18	66.22	64.21	67.08	64.39	63.54	66.28	73.24	65.82	63.47	65.49
Al_2O_3	13.09	14.14	20.77	18.85	18.24	13.92	13.90	14.61	20.74	20.58	18.86
FeO	0.06*	0.03*	–	–	–	0.14*	0.18*	0.23	–	–	–
MgO	–	6.24	–	–	–	–	9.34	1.69	–	–	–
CaO	11.32	0.20	3.56	0.10*	0.05*	10.71	0.16	0.19	2.74	0.07*	0.07*
SrO	–	–	–	2.83	–	–	–	–	–	5.63	–
BaO	–	–	–	–	6.69	–	–	–	–	–	5.67
Na_2O	10.58	11.70	9.93	10.33	9.74	9.88	8.73	9.22	9.23	9.00	8.95
K_2O	0.06*	0.16	0.43	0.05*	0.28	0.05*	0.11	0.07	0.06*	0.03*	0.05*
Cl	1.71	1.31	1.10	0.76	0.61	1.76	1.30	0.75	1.41	1.22	0.91
Total	100	100	100	100	100	100	100	100	100	100	100
A/CMSBNK**	0.344	0.398	0.892	0.942	0.875	0.389	0.362	0.736	1.025	1.005	1.010
ANCMSB/S**	0.761	0.738	0.741	0.656	0.669	0.740	0.716	0.517	0.688	0.710	0.640
CMSB**	4.23	3.22	1.30	0.60	0.95	4.00	4.76	0.92	1.00	1.17	0.81
SiO_2^{**}	65.56	67.75	69.73	73.50	72.75	66.15	66.64	77.07	71.18	70.65	73.31
CMSB/S**	0.192	0.144	0.059	0.026	0.042	0.181	0.213	0.037	0.045	0.053	0.035
Qtz	2.25	3.61	–	6.49	8.94	1.50	2.73	18.70	6.30	4.61	9.05
Or	–	0.96	2.57	–	1.67	–	0.60	–	–	–	–
Ab	68.63	72.86	81.98	83.43	69.87	73.02	72.00	75.97	79.33	77.21	76.56
An	–	–	10.95	–	–	–	–	–	13.81	–	–
$SrAl_2Si_2O_8$	–	–	–	8.95	–	–	–	–	–	17.96	–
$BaAl_2Si_2O_8$	–	–	–	–	16.48	–	–	–	–	–	14.03
Ne	–	–	1.61	–	–	–	–	–	–	–	–
Na_2SiO_3	5.25	6.40	–	1.12	3.04	2.86	0.71	0.67	–	–	–
Crn	–	–	–	–	–	–	–	–	0.56	0.22	0.36
Wo	23.88	0.42	2.89	–	–	22.62	0.34	0.40	–	–	–
En	–	15.75	–	–	–	–	23.63	4.26	–	–	–

Note: Average concentrations are given for 5–9 microprobe analyses for every experiment. All iron is in FeO form.
[1] Glasses from these experiments contain 5–10 vol % of crystals.
 * Concentrations below the analytical error (2σ).
** A/CMSBNK is the molar ratio $Al_2O_3/(CaO + MgO + SrO + BaO + Na_2O + K_2O)$; ANCMSB/S, atomic ratio $(Al + Na + Ca + Mg + Sr + Ba)/Si$; CMSB, $(Ca + Mg + Sr + Ba)$, at. %; SiO_2, concentration of SiO_2 in mol %; and CMSB/S, molar ratio $(CaO + MgO + SrO + BaO)/SiO_2$.

related to differences in the mechanisms of Cl incorporation in the structure of aluminosilicate melt. This resembles the two possible alternative mechanisms of chlorine dissolution in granodiorite melts proposed by Chevychelov (2003). It should be noted that the melts studied are very different in structural and physical characteristics, for instance, in the degree of polymerization.

There is no data in the literature on the solubility of chlorine in igneous melt at pressures below 0.5 kbar. Our study provides the first evidence for this pressure range, which is very interesting for interpretation of volcanic processes. In the compositions studied, chlorine solubility declined with decreasing pressure in the sequence 1.0–0.6–0.3–0.1 kbar. An increase in pressure from 1.0 to 3.0 kbar also reduced chlorine content in melt, which was clearly manifested in Ca-basalt and Ca-dacite with high chlorine contents. In experiments with Na-dacite containing 5.17 and 5.25 wt % CaO and albitite, similar chlorine concentrations were obtained at 1 and 2 kbar, whereas chlorine content decreased at $P = 3$ kbar. In the melts of Na-basalt and orthoclasite,

the concentrations of chlorine in quenched melts from experiments at 1, 2, and 3 kbar were identical within the uncertainty of microprobe analysis. Because of this, we believe that the pressure dependency of chlorine solubility in calcium-rich melts passes through a maximum at a pressure of about one kilobar (probably, 1–2 kbar for some compositions). It is known from the literature that there is a minimum on the Cl solubility curve at higher pressure (about 5–6 kbar). The decrease in chlorine solubility in aluminosilicate melt at increasing pressure between 1 and 5–6 kbar is probably related to rather large ionic radius of Cl$^-$. However, the reasons of the existence of the two extrema are unknown.

The results obtained in this study allow us to suggest that the solubilities of Cl and H_2O in aluminosilicate melts decline concurrently as pressure decreases below 1 kbar. An increase in pressure above 1 kbar results in an increase in H_2O solubility in aluminosilicate melt, whereas Cl solubility begins to decrease.

CONCLUSION

1. Chlorine solubility in the model melts at $T = 1250°C$ and $P = 0.1–3.0$ kbar varies from 0.2 to 4.7 wt %. The high chlorine solubility is related to a composite effect of melt compositions, high T, and relatively low P of experiments.

2. The composition of magmatic melt exerts a strong effect on the solubility of chlorine in it. For instance, at identical $P–T$ conditions, Cl content in the Ca-basalt melt is 10–15 times higher than in the melt of the orthoclase composition. In contrast, within a pressure interval from 100 to 3000 bar, Cl content varies much less significantly in glasses of similar compositions, by a factor of no higher than 1.5–2.0.

3. A maximum of chlorine solubility was found within the pressure range studied. It lies at ~1 kbar in the melts of Ca-basalt and Ca-dacite and at ~1–2 kbar in the melts of Na-dacite and albitite.

4. It was shown that the concentrations of bivalent alkali earth elements (especially, calcium) promote higher chlorine solubility in melt in comparison with the monovalent alkali elements. Chlorine solubility increases at the enrichment of melts in alkali earth elements in the sequences Ba–Sr–Ca and Mg–Ca. Chlorine solubility in sodium-rich aluminosilicate melt is higher than that in potassium-rich composition. The orthoclasite melt showed the lowest Cl contents among the compositions studied. They are about two times lower than those in the albitite melt.

5. The obtained quantitative data can be used for the construction of physicochemical models of ore systems, because chlorine is the most important complex-forming agent for the majority of metals.

REFERENCES

Chevychelov, V.Yu., Solubility of Chlorine in Fluid–Saturated Magmatic Melts with Granitoid Composition: The Effect of Calcium, *Geokhimiya*, 1999, no. 5, pp. 522–535.

Chevychelov, V.Yu. and Chevychelova, T.K., Partitioning of Pb, Zn, W, Mo, Cl, and Major Elements between Aqueous Fluid and Melt in the Systems Granodiorite (Granite, Leucogranite)–H_2O–NaCl–HCl, *Neues Jahrb. Miner. Abh.*, 1997, vol. 172, no. 1, pp. 101–115.

Chevychelov, V.Yu. and Epel'baum, M.B., Partitioning of Pb, Zn, and Major Components in the System Granitic Melt–Fluid, in *Ocherki fiziko-khimicheskoi petrologii* (Essays on Physicochemical Petrology), Moscow: Nauka, 1985, no. 13, pp. 120–136.

Chevychelov, V.Yu., Simakin, A.G., and Bondarenko, G.V., On the Mechanism of Chlorine Solution in a Model Water-Saturated Granodiorite Melt: The Use of Infrared Spectroscopy, *Geokhimiya*, 2003, no. 4 (in press).

Gorbachev, N.S. and Khodorevskaya, L.I., Partitioning of Chlorine between Hydrous Fluid and Basaltic Melts under High Pressures: Behavior of Chlorine and Water by Magmatic Degassing, *Dokl. Ross. Akad. Nauk*, 1995, vol. 340, no. 5, pp. 672–675.

Johannes, W. and Holtz, F., Petrogenesis and Experimental Petrology of Granitic Rocks, *Minerals and Rocks*, no. 22, Berlin: Springer, 1996.

Kadik, A.A., Lebedev, E.B., and Khitarov, N.I., *Voda v magmaticheskikh rasplavakh* (Water in Magmatic Melts), Moscow: Nauka, 1971.

Khodorevskaya, L.I. and Gorbachev, N.S., Experimental Study of Cu, Zn, Pb, Fe, and Cl Partitioning between Andesite and Water–Chlorine Fluid at High Parameters, *Dokl. Ross. Akad. Nauk*, 1993, vol. 332, no. 5, pp. 631–634.

Kilinc, I.A. and Burnham, C.W., Partitioning of Chloride between a Silicate Melt and Coexisting Aqueous Phase from 2 to 8 kbar, *Econ. Geol.*, 1972, vol. 67, no. 2, pp. 231–235.

Kravchuk, I.F. and Keppler, H., Distribution of Chloride between Aqueous Fluids and Felsic Melts at 2 kbar and 800°C, *Eur. J. Miner.*, 1994, vol. 6, pp. 913–923.

Kravchuk, I.F., Malinin, S.D., and Senin, V.G., Chlorine Solubility in Aluminosilicate Melts, *Geokhimiya*, 1998, no. 10, pp. 1065–1070.

Litvin, Yu.A., Ishbulatov, R.A., Chudinovskikh, L.T., *et al.*, Experimental Studies at High Pressures with Reference to the Problems of Mantle Magmatism, in *Eksperiment v resh-*

enii aktual'nykh zadach geologii (Experiment and Topical Problems of Geology), Moscow: Nauka, 1986, pp. 7–29.

Malinin, S.D. and Kravchuk, I.F., Behavior of Chlorine at Equilibria between Silicate Melt and Water–Chlorine Fluid, *Geokhimiya*, 1995, no. 8, pp. 1110–1130.

Malinin, S.D., Kravchuk, I.F., and Del'bov, F., Partitioning of the Chlorine Ion between Phases in Aqueous and "Dry" Systems of the Type Chloride–Aluminosilicate Melt Depending on Phase Compositions, *Geokhimiya*, 1989, no. 1, pp. 36–42.

Metrich, N. and Rutherford, M.J., Experimental Study of Chlorine Behavior in Hydrous Silicic Melts, *Geochim. Cosmochim. Acta*, 1992, vol. 56, pp. 607–616.

Shinohara, H., Iiyama, J.T., and Matsuo, S., Partition of Chlorine Compounds between Silicate Melt and Hydrothermal Solutions: I. Partition of NaCl–KCl, *Geochim. Cosmochim. Acta*, 1989, vol. 53, no. 10, pp. 2617–2630.

Suk, N.I., Behavior of Ore Elements (W, Sn, Ti, and Zr) in Immiscible Silicate–Salt Systems, *Petrologiya*, 1997, vol. 5, no. 1, pp. 23–31.

Webster, J.D., Exsolution of Magmatic Volatile Phases from Cl-Enriched Mineralizing Granitic Magmas and Implications for Ore Metal Transport, *Geochim. Cosmochim. Acta*, 1997, vol. 61, no. 5, pp. 1017–1029.

Webster, J.D., Fluid–Melt Interactions Involving Cl-Rich Granites: Experimental Study from 2 to 8 kbar, *Geochim. Cosmochim. Acta*, 1992a, vol. 56, pp. 659–678.

Webster, J.D., Water Solubility and Chlorine Partitioning in Cl-Rich Granitic Systems: Effects of Melt Composition at 2 kbar and 800°C, *Geochim. Cosmochim. Acta*, 1992b, vol. 56, pp. 679–687.